EXPERIMENTAL AND NUMERICAL ANALYSIS OF GAS MOTION IN A STANDARD COOPERATIVE FUEL RESEARCH ENGINE

Charles Rech, charlesrech@uol.com.br
Flavio V Zancanaro Jr, zancanaro@mecanica.ufrgs.br
Fabiano Disconzi Wildner, wildner66@yahoo.com.br
Mechanical Engineering Graduate Program, Federal University of Rio Grande do Sul, Brazil

Horácio A Vielmo, vielmoh@mecanica.ufrgs.br
Mechanical Engineering Department, Federal University of Rio Grande do Sul, Brazil

Amir A M Oliveira Jr, amir.oliveira@gmail.com
Mechanical Engineering Department, Federal University of Santa Catarina, Brazil

Abstract. *This paper focuses on a transient flow that occurs in the intake system and in-cylinder of a standard CFR (Cooperative Fuel Research) engine. The engine under consideration has a bore of 82.55 mm and a stroke of 114.30 mm. As a first step the engine has no combustion, but is driven by an electrical motor that provides the desired angular velocity, in this case 200 rpm. Numerical solutions using a commercial Finite Volumes CFD code are performed, applying moving hexahedral trimmed meshes, and compared with experimental results of air flow in the intake system. Regarding turbulence, computations were performed with Reynolds-Averaged Navier-Stokes, Eddy Viscosity Models k-ω SST, in its Low Reynolds approach with hybrid treatment near the walls. Convergence tests were performed and a secure criterion established. The enthalpy equation is also solved and the air is treated as a perfect gas, taking compressibility into account. A mesh independence study was performed, through discharge coefficient in the maximum piston velocity, at 75 degrees after top dead center. The presence of recirculation at the port and inside the cylinder is detected and discussed in detail. The results revealed the formation of swirl and also showed the evolution of the flow field and the variation of swirl ratios as important information for the design intake and exhaust systems of internal combustion engines.*

Keywords: CFR engine, CFD, turbulence models, experimental validation

1. INTRODUCTION

The research of lean burn engines has become important to reduce the emissions and fuel consumption. However, when developing engines, the gas motion sometimes is not fully analyzed, requiring many experiments with many trial productions of intake ports and combustion chambers. To meet more and more stringent emissions requirements, many advanced techniques, such as lean burn, multivalves, swirling and tumble flow are adopted in SI engines. These techniques are closely related with the in-cylinder gas motion generated during the intake process. Swirl can promote fuel atomization, evaporation and mixing.

The discharge coefficient measures the flow permeability in the engine intake system. Deep and detailed research on the in-cylinder gas flow produced during the intake process is helpful for achieving its efficient control and utilization in order to improve combustion, enhance performance and reduce emissions when developing engines.

The burning rate, as Baritaud (1989) has shown, can be directly related to the turbulence intensity generated by swirl. It appears that increased turbulence during combustion corresponds to an increase in flame kernel growth rate and turbulent flame speed. Swirl accelerate the flame kernel growth rate and cyclic variation can then be substantially reduced (Witze *et al.*, 1988; Lord *et al.*, 1993; Aucoumanis *et al.*, 1998; Ancimer *et al.*, 1999; Selamet *et al.*, 2004). Mikulec *et al.* (1988) found the least standard deviation of peak cylinder pressure with the maximum rotating speed of swirl. Swirl affect thermal efficiency of engines due to reduced ignition delay, increased heat transfer to the combustion chamber walls, and decreased volumetric efficiency (Davis and Borgnakke, 1982; Alkidas *et al.*, 1990; Zhang and Frankel, 1997). The potential to reduce specific fuel consumption is the net result of a number of effects. The net effect of swirl on the thermal efficiency depends on several effects including swirl intensity, mixture strength, ignition source, and combustion chamber configuration (Hill and Zhang, 1994). Swirl can be effective to improve the thermal efficiency of SI engines.

With the rapid progress of computer performance, the three-dimensional computational fluid dynamics (CFD) has become applicable to engine analysis (Barata 2003, Barata2008a,b, and c, Barata 2009 and Zancanaro 2010).

During the last few years more numerical simulations have been performed regarding swirl and discharge coefficients (Bianchi et al., 2002a, 2003), focusing in directed intake port types, including comparisons with experimental measurements. With the growing availability of turbulent models and computational resources, many articles made comparisons regarding ability to reproduce experimental data and CPU time demands.

Kaario et al. (2003) compared the k-ε RNG turbulence model with the one-equation subgrid scale model, incompressible and isothermal LES approach (Large Eddy Simulation). This particularized form of the LES model was

able to capture more flow complex structures than the k-ε RNG model (k-ε Renormalization Group), but remains with the problem of large CPU time demand.

Keeping the popular k-ε family, some works have been analyzing the alternatives for the stress-strain relationship, considering the compressible, non-isothermal, anisotropic effects presents in the ICE (Internal Combustion Engine) three-dimensional flows. Bianchi at al. (2002b, 2003) compared k-ε linear and nonlinear (quadratic and cubic) eddy viscosity models, concluding that cubic stress-strain relations provided the best agreement with the experimental data, for those ICE three-dimensional flows considered. In another work (2003) the same author investigated the High Reynolds and Low Reynolds near wall approaches, both with a cubic relationship between Reynolds stresses and strains. It was concluded that the Low Reynolds approach (boundary layer also discretized by the mesh), although increasing the computational effort, presented more ability in capturing the tested ICE intake flow.

In this work, comparisons between predictions and measurement of air flow in the intake system are made and show good agreement with experimental data from a CFR engine and the results obtained by the numerical solutions using a commercial Finite Volumes CFR revealed the formation of swirl motion and the evolution of flow, pressure and temperature fields.

2. MATHEMATICAL MODEL

The velocity field is described by the mass and momentum conservation equations (Navier-Stokes), in their transient, compressible form.

In Cartesian tensor notation, according Warsi (1981), the mass conservation is

$$\frac{\partial \rho}{\partial t} + \frac{\partial}{\partial x_j}\left(\rho u_j\right) = 0 \tag{1}$$

and the momentum

$$\frac{\partial \rho u_i}{\partial t} + \frac{\partial}{\partial x_j}\left(\rho u_j u_i - \tau_{ij}\right) = -\frac{\partial p}{\partial x_i} + s_i \tag{2}$$

being p the piezometric pressure defined:

$$p = p_s - \rho_0 g_m x_m \tag{3}$$

where p_s is static pressure, ρ_0 is reference density, g_m the are gravitational acceleration components and the x_m are coordinates relative to a datum where ρ_0 is defined.

As the fluid is Newtonian, and the flow is turbulent, assuming the ensemble average (equivalent to time averages for steady-state situations), the stress tensor components are, according Hinze (1975),

$$\tau_{ij} = 2\mu\, S_{ij} - \frac{2}{3}\mu \frac{\partial u_k}{\partial x_k}\delta_{ij} - \overline{\rho u_i' u_j'} \tag{4}$$

and strain tensor

$$S_{ij} = \frac{1}{2}\left(\frac{\partial u_i}{\partial x_j} + \frac{\partial u_j}{\partial x_i}\right) \tag{5}$$

The *u'* are fluctuations about the ensemble average velocity, and overbar denotes the ensemble averaging process. Finally, as the flow is compressible and non-isothermal, in the Eq. (2)

$$s_i = g_i\left(\rho - \rho_0\right) \tag{6}$$

where g_i is the gravitational acceleration component in x_i direction. Considering the air as an ideal gas

$$\rho = \frac{p}{RT} \tag{7}$$

For the heat transfer problem, the enthalpy equation is also solved. According Jones (1980),

$$\frac{\partial \rho h}{\partial t} + \frac{\partial}{\partial x_j}\left(\rho h u_j + F_{h,j}\right) = \frac{\partial p}{\partial t} + u_j \frac{\partial p}{\partial x_j} + \tau_{ij}\frac{\partial u_i}{\partial x_j} \tag{8}$$

where $h = \overline{c}_p T - c_p^0 T_0$ is the static enthalpy; $\overline{c}_p$ is the mean constant-pressure specific heat at temperature T; c_p^0 the reference specific heat at temperature T_0, and $F_{h,j}$ the diffusional energy flux in direction x_j, given by

$$F_{h,j} \equiv -k_t \frac{\partial T}{\partial x_j} + \overline{\rho u_i' h'} \tag{9}$$

where k_t is the thermal conductivity.

2.1 Constitutive Relations

The rightmost terms of the Eq. (4) and Eq. (9) represents the additional Reynolds stresses due to turbulent motion. These are linked to the mean velocity field via turbulence models. According Launder and Spalding (1974), for linear viscosity models

$$-\overline{\rho u_i' u_j'} = u_t S_{ij} - \frac{2}{3}\left(u_t \frac{\partial u_k}{\partial x_k} + \rho k\right)\delta_{ij} \tag{10}$$

and

$$-\overline{\rho u_i' h'} = -\frac{\mu_t}{\sigma_{h,t}}\frac{\partial h}{\partial x_j} \tag{11}$$

where $k = \overline{u_i' u_i'}/2$ is the turbulence kinetic energy; μ_t the turbulent viscosity; $\sigma_{h,t}$ the turbulent Prandtl number and

$$S_{ij} = \frac{\partial u_i}{\partial x_j} + \frac{\partial u_j}{\partial x_i} \tag{11}$$

2.2 Governing Equations for the SST *K-ω* Turbulence Model

The specific dissipation rate is defined as $\omega = \varepsilon / C_\mu k$, and the general form of the turbulent kinetic energy is

$$\frac{\partial}{\partial t}\left(\rho k\right) + \frac{\partial}{\partial x_j}\left[\rho u_j k - \left(\mu + \frac{\mu_t}{\sigma_k^\omega}\right)\frac{\partial k}{\partial x_j}\right] = \mu_t P - \rho\beta^* k\omega + \mu_t P_B \tag{12}$$

and specific dissipation rate is

$$\frac{\partial}{\partial t}\left(\rho\omega\right) + \frac{\partial}{\partial x_j}\left[\rho u_j \omega - \left(\mu + \frac{\mu_t}{\sigma_\omega^\omega}\right)\frac{\partial \omega}{\partial x_j}\right] = \alpha\frac{\omega}{k}\mu_t P - \rho\beta\omega^2 + \rho S_\omega + C_{\varepsilon 3}\mu_t P_B C_\mu \omega \tag{13}$$

where $C_{\varepsilon 3}$=0.0 or 1.44 if $P_B > 0$ and C_μ=0.09 are empirical coefficients. For the SST k-ω model the other coefficients are given in Menter (1993).

3. NUMERICAL METHODOLOGY

Numerical transient solutions using the commercial Finite Volumes CFD code StarCD es-ice were performed, for a CFR engine. A user defined unstructured hexahedral-trimmed cells moving mesh was constructed, as showed in the Fig. 1 and Fig 2. A mesh independence study was performed, arriving in 13452482 cells in the domain (Fig. 3). Regarding the turbulence, it is applied the k-ω SST model in Low-Reynolds approach, with hybrid near wall treatment. All computations were performed with double precision. The pressure-velocity coupling is solved thought the SIMPLE algorithm. The used differencing scheme is the Linear Upwind Differencing (LUD), with blending factor (bf) of 0.3 for the momentum, turbulence and enthalpy equations and bf = 0.1 for pressure. For the density, the Central Differencing (CD), with bf = 0.3 , was applied.

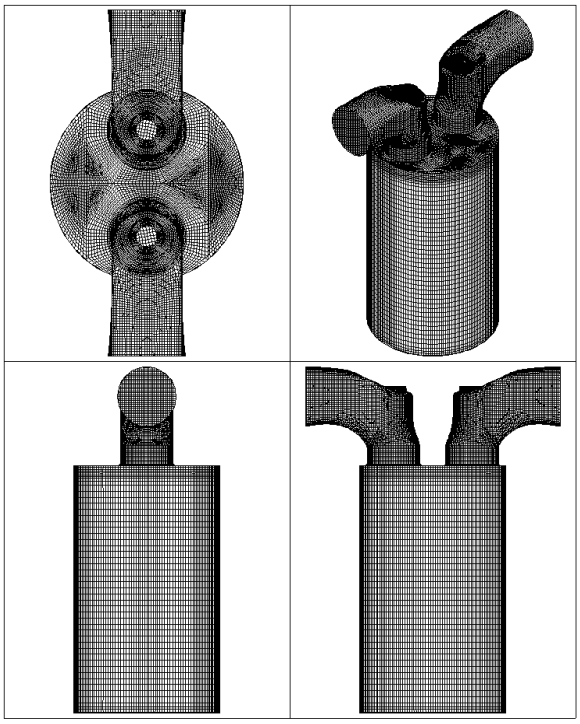

Figure 1 - Unstructured hexahedral-trimmed cells moving mesh

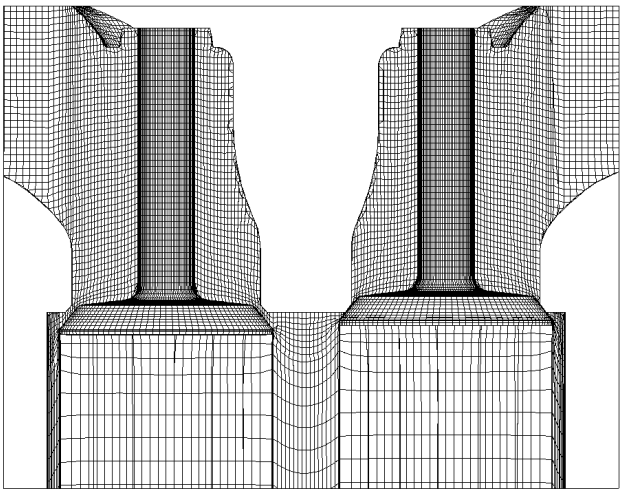

Figure 2 –Unstructured hexahedral-trimmed cells moving mesh detail

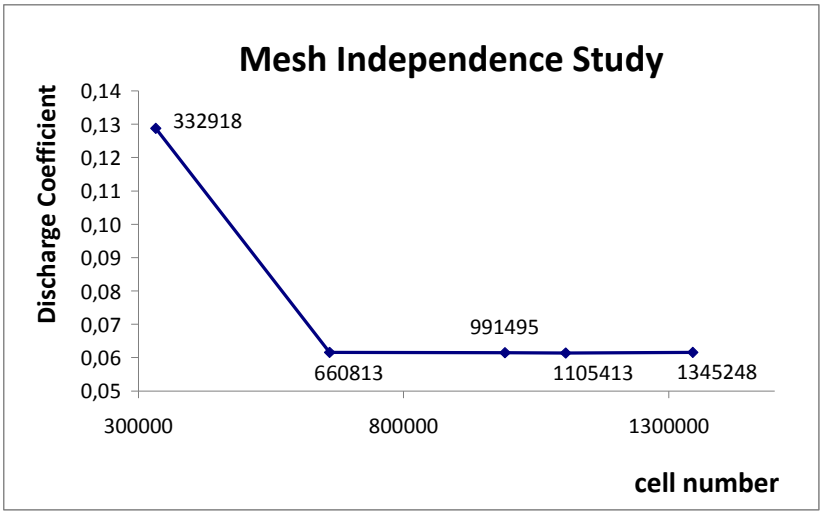

Figure 3 - Mesh independence study for the maximum piston velocity, at 75 degrees after top dead center

4. BOUNDARY AND INITIAL CONDITIONS

The boundary conditions are stagnation pressure (p_{st}) of 1 *atm* at the inlet, with 293.15 K, discharging in an ambient pressure (p_{out}) of 1 *atm*, and 293.15 K. For all cases the turbulence boundary conditions are turbulence intensity $I = 0.05$, and length scale $l = 0.0034$ m, as a consequence of the flow and geometrical characteristics. Regarding the heat transfer problem, considering a cold flow (exhaust and compression processes, without combustion), the cylinder wall and piston crown have a constant temperature of 400 K, and a thermal resistance of 0.004 m^2K/W. Accordingly, for the combustion chamber dome, values are 450 K and 0.004 m^2K/W. For intake and exhaust valves and ports the temperature is 350 K and thermal resistance is 0.004 m^2K/W.

As initial condition for the independency mesh analysis, the crankshaft starts at 360º, almost at the end of the exhaust process. All the velocity components inside the cylinder are set to 0.1 m/s, at 1 *atm* and 300 K. For the rest of the simulation, the initial conditions are the final values of the previous cycle.

5. THE DISCHARGE COEFFICIENT

The impact of a blockage on engine breathing is assessed through a discharge coefficient C_D that relates the actual mass flow rate through the intake valve to the isentropic mass flow rate. Therefore, the equation assumes the following form (Heywood, 1988; Ferrari ,2005).

$$C_{D\_actual} = \frac{\dot{m}_{actual}}{\frac{\pi d_V^2}{4}\frac{p_{st}}{\left(RT_o\right)^{1/2}}\left(\frac{p_{out}}{p_o}\right)^{1/\gamma}\left\{\frac{2\gamma}{\gamma-1}\left[1-\left(\frac{p_{out}}{p_o}\right)^{(\gamma-1)/\gamma}\right]\right\}^{1/2}} \tag{14}$$

where $\dot{m}_{actual}$ is obtained from the numerical solution, or experimentally, R is the gas (air) constant, T_o the stagnation (inlet) absolute temperature, d_v is the inner valve diameter and γ the specific heat ratio.

6. THE SWIRL RATIO (R_S)

The swirl motion pattern describes the rotation of the in-cylinder charge around the cylinder axis. The swirl ratio, R_s, is a normalized value used to show the motion pattern of the rotating fluid within the cylinder. Assuming that the flow inside the cylinder is a solid body rotational flow, the swirl ratio is obtained by dividing the rotational angular velocity (ω_s) by the crankshaft rotational velocity, as follows (Heywood, 1988; Star_CD methodology ,2009).

$$R_s = \frac{\omega_s}{\left(2\pi N\right)/60} \tag{15}$$

where N is the angular speed of engine. Then, the swirl ratio for the non rigid (air) real situation is computed as:

$$R_S = \frac{\sum_{cells} \rho_i V_i \left[\left(x_i - x_m \right) v_i - \left(y_i - y_m \right) u_i \right]}{2\pi \frac{N}{60} I_z} \tag{16}$$

where x_i, y_i and z_i are the centroid coordinates of cell i; x_m, y_m and z_m are the centre of mass coordinates; v_i and u_i are velocity components, ρ_i is the density, V_i is the volume of cell i and I_z is the moment of inertia, which can be computed as follows:

$$I_z = \sum_{cells} \rho_i V_i \left(\left(y_i - y_m \right)^2 + \left(x_i - x_m \right)^2 \right) \tag{17}$$

7. EXPERIMENTAL METHODOLOGY

Experimental measurements in the intake system were made on a single cylinder four stoke motored CFR engine. The specifications of the engine are given in the Table 1.

Table 1. Specifications of the CFR engine

ASTM-CFR - engine	
Bore x Stroke (mm)	82.55 x 114.30
IVO/IVC (ATDC)	0 / 202
Displacement (cm^3)	611.30
Maximum valve lift (mm)	6.05
Intake air system	Naturally aspirated
Compression ratio	6:1

To experimental date the engine was instrumented with data acquisition, angular position and air flow measurement. The angular position of the crankshaft was measured with an incremental encoder (Danaher Sensors & Controls, model BA 3022). The encoder was connected to the crankshaft and supplied 1733.33 pulses per revolution, with a resolution of 0.20769 degrees. The mass air flow was measured with an automotive hot film anemometer. (MAF -Bosch 0 280 218 002). The data was acquired with a commercial data acquisition board (National instruments 6124) and its original software LabView. The values of voltage and frequency were collected and processed with the correspondent calibration curves of each sensor and converted into units of mass flow and angular position. It was acquired 6000 samples for second.

8. RESULTS AND DISCUSSION

Flow fields generated during the intake stroke of the motored engine were studied experimentally and numerically. Increasing intake restriction by the partially opened valve is associated, in general, with reduced C_D, hence lowered engine breathing capacity. The intake discharge coefficient C_D, calculated from Eq. (14), is presented in Fig. (4). This result was obtained from the division of the numerical, quasi-static and measured data of mass air flow by the isentropic values of Eq. (14), with specific heat ratio γ=1.4. As shown in the Fig. (4), a good agreement is verified among the results.

After the opening of the intake valve, starts the intake phase of air in the engine. It was verified that the maximum intake discharge coefficient occurs around 75 degrees of the intake phase. The maximum experimental discharge coefficient value is close to the quasi-static and numerical values. The experimental data of mass flow had been collected in hot wire anemometer sensor at 15 cm of the intake port, and converted into the coefficient of discharge by Eq. (14). The numerical data had been computed in the intake port. It has, therefore, a physical distance from the place of the collection to the numerical and experimental data. Although the angular velocity of the engine was low, the inertia effects are already present.

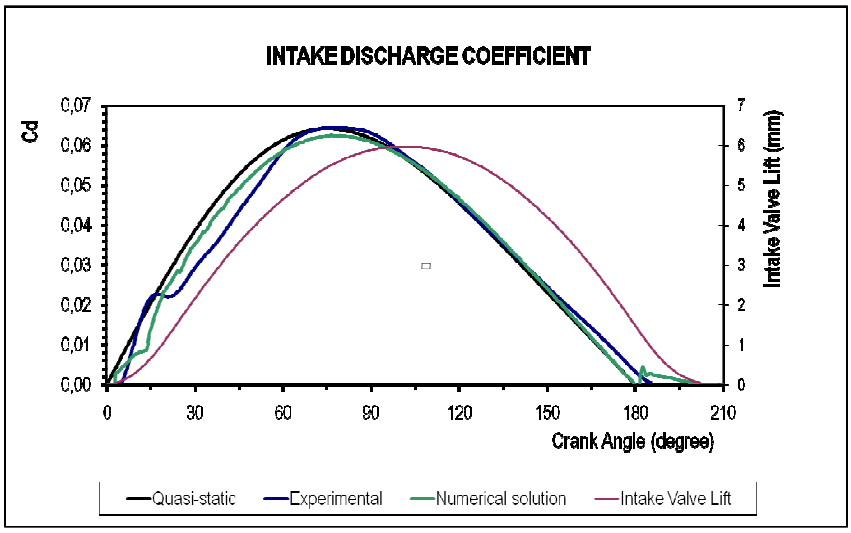

Figure 4. Intake discharge coefficient for 200 rpm

As seen on Fig. (4), there is a discontinuity in the curve at the beginning intake process, around 20 degrees, for experimental and numerical results. In this point the total volume of the intake system is of 55268 mm^3, where there are 129647 mesh cells. The average volume for each cell is 0.43 mm^3 and, considering a perfect hexahedron, its edge is around 0.75 mm. The average speed in the intake system is about 5 m/s for a time step of 0.2 degrees ($1.66E^{-4}$ s) in the rotation of 200 rpm. Considering the speed of the sound 347 m/s, the Courant Number (that relates the speed of propagation of the information with the size of the mesh), is around 860. For Courant = 1, the time step must be of the order of $2.2E^{-6}$ s. The conclusion is that the inertial effect would not be caught as waves of compression and expansion of air, but maybe as transient variations, attenuated for the insufficiency of the time step.

Figures 5 and 6 show the velocity fields at 75°, for the time step 0.2°, piston velocity of 1.25 m/s in the X-Z plane, i.e., the plane parallel to the cylinder axis and normal to the line from the intake valve to the exhaust valve. At this point, the fluid flow is driven through inlet port, as a strong annular conical jet, generating regions with different patterns inside the cylinder. It is detected a large recirculating flow, and on the intake valve seat there is a detachment, caused by low pressure downstream the valve plate. These characteristics of detachment and recirculating flow at the intake valve are confirmed by the literature (Heywood 1988, Ferrari 2005) as a consequence of the intake valve geometry. Because of the restrictions at the valve plate, this is the region of highest velocities and friction. Indeed, this restriction causes almost all of the pressures losses of the expansion.

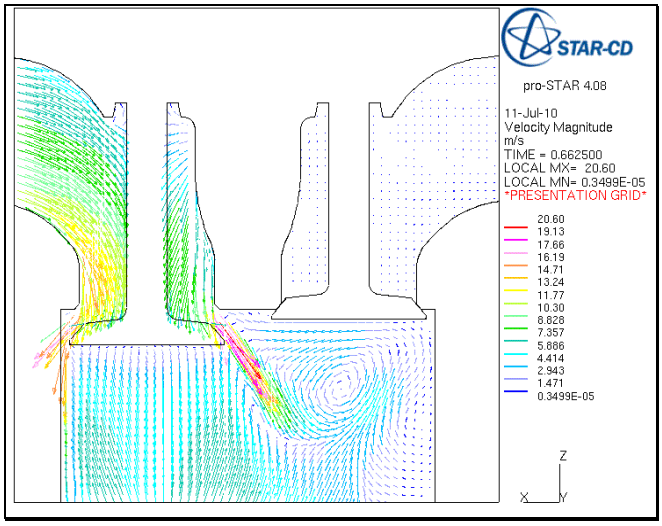

Figure 5 - Velocity vectors field at, 75° ATDC, for the time step of 0.2°, piston velocity of 1.25 m/s, in the X-Z plane.

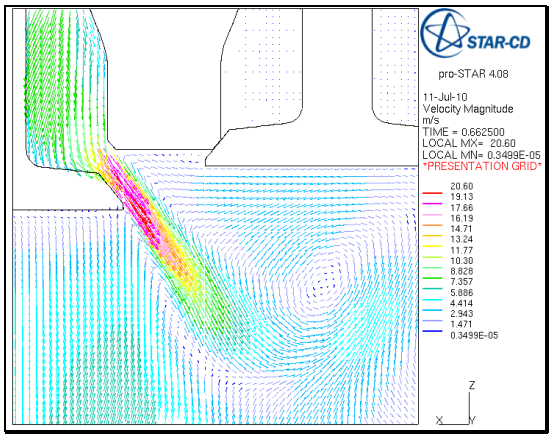

Figure 6 - Velocity vectors field detail at intake seat valve, 75° ATDC, for the time step of 0.2°, piston velocity of 1.25 m/s, in the X-Z plane.

The Figs. 7 and 8 show the absolute pressure field in the X-Z plane. It is possible to observe that the lowest values are concentrated around the intake valve plate because of high velocities, and inside cylinder. There is also a partial recovery of pressure in a region near the piston, due to velocity reduction.

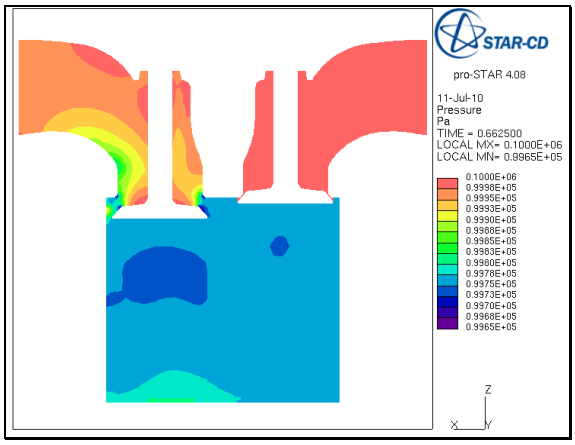

Figure 7 – Pressure field at 75° ATDC, for the time step of 0.2°, piston velocity of 1.25 m/s, in the X-Z plane

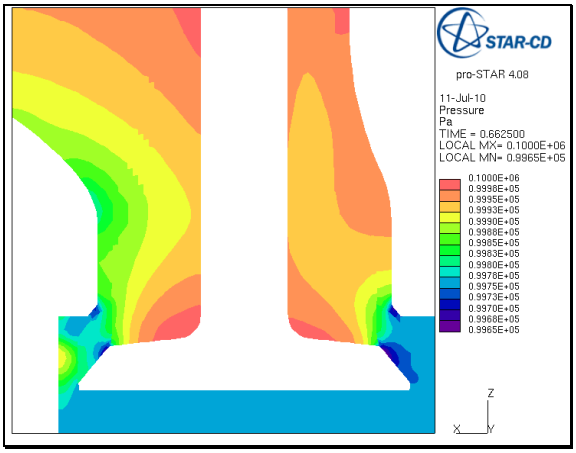

Figure 8 – Pressure field detail at seat valve, 75° ATDC, for the time step of 0.2°, piston velocity of 1.25 m/s, in the X-Z plane.

Considering the good agreement between the experimental and numerical results for the discharge coefficient, another important common fluid flow pattern was investigated, the swirl motion. The Fig. 9 shows the results for the swirl ratio as a function of the crank angle. During the intake stroke, after TDC, its value increases progressively and continues during the compression stroke. The negative value indicates that the resultant of the fluid rotation is clockwise. The swirl ratio reaches its maximum at 197° ATDC, and decreases until 360°.

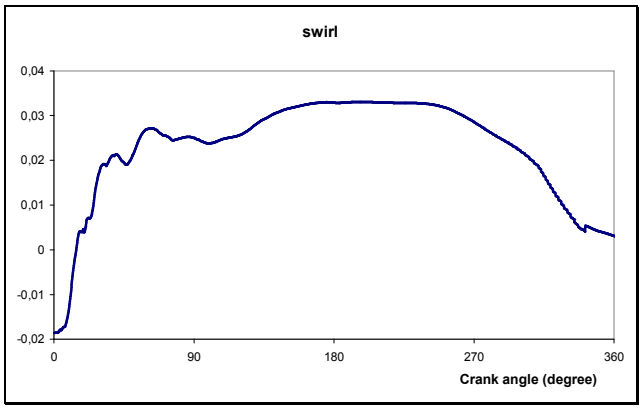

Figure 9. Swirl obtained by numerical solution, 200 *rpm*

9. CONCLUSION

In order to precisely predict the in-cylinder flow field of a CFR engine, numerical and experimental methodology were employed for studying the 3D turbulent transient compressible flow at 200 rpm. Comparisons were made between the simulation and experimental measurements.

The simulation demonstrates good agreement with measured values.

One verifies that the discharge coefficient increases with increasing lift, however early in relation to crank angle. The air flow rate through the intake valve varies with pressure expansion ratio, increasing as the pressure expansion ratio increases, as expected.

The swirl ratio increases at intake processes and reaches its maximum at 197° ATDC decreasing until 360°. The negative value indicates that the resultant of the fluid rotation is clockwise.

On the intake valve plate there is a detachment, followed by a recirculation zone, due to inertial forces and intake valve and duct geometry.

For all the situations investigated, the presence of recirculation in the port and in-cylinder are detected.

10. ACKNOWLEDGEMENTS

The authors thank the financial support from CAPES and CNPq, Brazil, for the Graduate Scholarships to Rech, C., Zancanaro, F.V.Jr. and Wildner, F.D. Also for the CNPq scientific productivity grant to Vielmo, H.A. and the CNPq Universal Project 475237/2009-9.

11. REFERENCES

Alkidas, A. C., Puzinauskas, P. V., and Peterson, R. C., 1990, "Combustion and heat transfer studies in a spark-ignited multivalve optical engine", SAE Paper 900353.

Ancimer, R., Jaaskelainen, H., and Wallace, J., 1999, "Experiments into the flame kernel development in high swirl production spark ignition engines", SAE Paper 1999-01-3544.

Arcoumanis, C., Godwin, S.N., and Kim, J.W., 1998, "Effect of tumble strength on exhaust emissions in a single cylinder 4-valve S.I engine", SAE Paper 981044.

Baratta, M., Catania, A.E., Spessa, E., and Liu, R.L., 2003, "Multidimensional Predictions of In-Cylinder Turbulent Flows: Contribution to the Assessment of k-ε Turbulence Model Variants for Bowl-In-Piston Engines". ASME J. of Eng. Gas Turbines Power, 127, pp. 883-896.

Baratta, M.; Catania, A.E.; d´Ambrosio, S., 2008c, "Nonlinear Versus Linear Stress-Strain Relations in Engine Turbulence Modeling Under Swirl and Squish Flow Conditions", ASME paper, Journal of Engineering for Gas Turbines and Power, vol. 130: pp. 062802-1-062802-11.

Baratta, M.; Catania, A.E.; Pesce, F.C.; Spessa, E.; Rech C.; Vielmo, H.A., 2008a, "Multidimensional Modeling of a High Swirl-Generating Helical Intake Port for Diesel Engines", 12th Brazilian Congress of Thermal Engineering and Sciences, Belo Horizonte -MG, Proceedings of ENCIT, Rio de Janeiro, RJ: ABCM.

Baratta, M.; Catania, A.E.; Pesce, F.C.; Spessa, E.; Rech, C.; Vielmo, H.A., 2008b, "Comparisons Between Steady State Analyses of a High Swirl-Generating Helical Intake Port for Diesel Engines", 12th Brazilian Congress of Thermal Engineering and Sciences, Belo Horizonte - MG. Proceedings of ENCIT, Rio de Janeiro, RJ: ABCM.

Baratta, M.; Catania, A.E.; Pesce, F.C.; Spessa, E.; Rech, C.; Zancanaro, F.V.Jr; Vielmo, H.A., 2009, "Transient Numerical Analysis of a High Swirled Diesel Engine", 20th International Congress of Mechanical Engineering, Gramado – RS, Proceedings of COBEM, Rio de Janeiro, RJ: ABCM.

Baritaud, T. A. ,1989, "Combustion and fluid dynamic measurements in a spark-ignition engine - Effects of thermochemistry and velocity field; turbulent flame speeds", SAE Paper 892098.

Bianchi, G.M., Cantore, G. and Fontanesi, S., 2002a, "Turbulence Modeling in CFD Simulation of ICE Intake Flows: The Discharge Coefficient Prediction". SAE Paper N^{o} 2002-01-1118.

Bianchi, G.M., Cantore, G., Parmeggiani, P. and Michelassi, V, 2002b, "On Application of Nonlinear k-ε Models for Internal Combustion Engine Flows". Transactions of the ASME vol. 124, pp. 668-677.

Bianchi, G.M., Fontanesi, S., 2003, "On the Applications of Low-Reynolds Cubic k-ε Turbulence Models in 3D Simulations of ICE Intake Flows". SAE Paper No 2003-01-0003.

Davis, G. C. and Borgnakke, C., 1982, "The effect of in-cylinder flow processes (swirl, squish and turbulence intensity) on engine efficiency - model predictions", SAE Paper 820045.

Ferrari, G., 2005, "Motori a Combustione Interna", Torino, Ed il Capitello, (in italian).

Heywood, J.B., 1988, "Internal Combustion Engines". McGraw-Hill Inc.

Hill, P. G. and Zhang, D., 1994, "The effect of swirl and tumble on combustion in sparkignition engines". Prog. Energy Combust. Sci., 20:373-429.

Hinze, P.O., 1975, "Turbulence", 2nd Edition, McGraw-Hill, New York.

Jones, W.P., 1980 "Prediction Methods for Turbulent Flow, Hemisphere", Washington, D.C., pp. 1-45.

Kaario, O.; Pokela, H.; Kjaldman, L.; Tiainen, J.; Larmi, M. LES and RNG Turbulence Modeling in DI Diesel Engines, SAE paper N°. 2003-01-1069, 2003.

Launder, B.E. and Spalding, D.B., 1974 "The Numerical Computation of Turbulent Flows, Computational Methods in Applied Mechanics and Engineering", 3, pp. 269-289.

Lord, D. L.; Anderson, R. W.; Brehob, D. D.; Kim, Y. "The effects of charge motion on early flame kernel development", SAE Paper 930463, 1993.

Menter, F.R., 1993 "Zonal Two Equation k-ω Turbulence Models for Aerodynamic Flows" Proc. 24th Fluid Dynamics Conf., Orlando, Florida, USA, Paper No. AIAA 93-2906.

Mikulec, A., Kent, J. C., Adamczyk, A. A., and Rimai, L., 1988, "Effects of intake port configuration on induction-generated swirl in a piston engine: a water analog experiment using particle tracking velocimetry", 2nd International Symposium on Fluid Control, Measurement, Mechanics, and Visualization, Sheffield University, England.

Selamet, A., Rupai, S., and He, Y., 2004, "An experimental study on the effect of intake primary runner blockages on combustion and emissions in SI engines under part-load conditions", SAE Paper 2004-01-2973.

Star-cd Version 4.10. Methodology, CD-adapco, 2009.

Warsi, Z.V.A., 1981, "Conservation Form of the Navier-Stokes Equations in General Nonsteady Coordinates", AIAA Journal, 19, pp. 240-242.

Witze, P. O., Hall, M. J., and Wallace, J. S., 1988, "Fiber-optic instrumented spark plug for measuring early flame development in spark ignition engines", SAE Paper 881638.

Zancanaro, F V.Jr., 2010, "Simulação Numérica do Escoamento Turbulento em Motores de Combustão Interna", Promec, UFRGS.

Zhang, D. H. and Frankel, S. H., 1997, "Optimization of natural gas engine performance by multidimensional modeling", SAE Paper 971567.

12. RESPONSIBILITY NOTICE

The authors are the only responsible for the printed material included in this paper.